Bioorganic & Medicinal Chemistry 18 (2010) 5510–5518

Contents lists available at ScienceDirect

Bioorganic & Medicinal Chemistry

journal homepage: www.elsevier.com/locate/bmc

New chloro,fluorobenzylindole derivatives as integrase strand-transfer inhibitors (INSTIs) and their mode of action

Stefania Ferro [a], Laura De Luca [a,*], Maria Letizia Barreca [b], Sara De Grazia [a], Frauke Christ [c], Zeger Debyser [c], Alba Chimirri [a]

[a] Dipartimento Farmaco-Chimico, Università di Messina, Viale Annunziata, I-98168 Messina, Italy
[b] Dipartimento di Chimica e Tecnologia del Farmaco, Università di Perugia, Via del Liceo, 1, I-06123 Perugia, Italy
[c] Molecular Virology and Gene Therapy, Molecular Medicine, Katholieke Universiteit Leuven and IRC KULAK, Kapucijnenvoer 33, B-3000 Leuven, Flanders, Belgium

ARTICLE INFO

Article history:
Received 11 February 2010
Revised 11 June 2010
Accepted 16 June 2010
Available online 22 June 2010

Keywords:
HIV-1 integrase
Induced-fit docking
Integrase strand-transfer inhibitors
Microwave-assisted organic synthesis

ABSTRACT

The life cycle of HIV-1 requires extensive assistance from the integrase (IN) enzyme which therefore constitutes an attractive therapeutic target for the development of anti-AIDS agents. We herein report the synthesis and biological evaluation of new HIV integrase strand-transfer inhibitors (INSTIs) which proved to be also potent anti-HIV agents. The binding mode of the most representative molecules were also studied by induced-fit docking (IFD). The obtained IFD results were consistent with the mechanism of action proposed for this class of IN inhibitors, that is metal chelating/binding agents.

1. Introduction

AIDS (Acquired immune deficiency syndrome), caused by Human Immodeficiency Virus (HIV), is a severe infectious disease responsible for a large number of deaths every year. Studies in HIV biology have provided important information about the main steps of the virus life cycle which consists of viral entry, reverse transcription, integration, gene expression, virion assembly, budding and maturation. The officially approved drugs belong to the class of reverse transcription and protease inhibitors and, recently, viral entry and integrase inhibitors.

Despite the successes with such treatments as HAART (highly active antiretroviral therapy) combination regimens, the permanent use of anti-AIDS drugs induces drug-resistant viral variants and emergence of unwanted metabolic side effects.[1]

In addition, some data have shown that HIV can survive in extremely long-living cells and be reactivated even after years of HAART regimens.[2] Therefore, the discovery and the development of new more potent and less toxic anti-HIV agents capable of suppressing drug-resistant HIV strains and/or targeting different stages in the virus life cycle are still warranted.

Considering that successful completion of the HIV-1 viral life cycle depends in part on the integration of complementary DNA mediated by HIV-1-Integrase (IN) and also that there is no known human counterpart,[3] this essential enzyme might constitute a therapeutically highly advantageous target.[4]

IN catalyzes the insertion of HIV-1 DNA into the genome of the host cell through a multistep process which includes the following different biochemical steps: (i) assembly of a stable complex with specific DNA sequences at the end of the HIV-1 long terminal repeat (LTR) regions, (ii) endonucleolytic processing of the viral DNA to remove the terminal dinucleotide from each 3′ end (3′P), and (iii) strand-transfer (ST) in which the viral DNA 3′ ends are covalently legated to the host chromosomal DNA. No energy source (e.g., ATP) is needed for the integration reaction, and only divalent cations are required for catalytic activity.[5,6]

In particular, the two metal cofactors of HIV IN are thought to both be Mg^{2+} ions under physiological conditions. Even if the exact mechanism of action of IN inhibitors has not been completely elucidated, it is believed that the inhibitors of the IN stand transfer (INSTIs) step bind to the acceptor DNA site of the enzyme and act by sequestering the metal ions bound in the IN active site to form a ligand–M^{2+}–IN complex.[7–9]

Moreover, it has been demonstrated that INSTIs bind at the IN–DNA interface rather than to IN alone,[10,11] thus acting as interfacial inhibitors of protein–nucleic acid interactions.[12,13]

Research has focused on the molecular binding of INSTIs to integrase complexes because of the increasing importance of selective INSTIs as antiviral compounds and of their unique mechanism of action.[12]

* Corresponding author. Tel.: +39 0906766464; fax: +39 0906766402.
E-mail address: ldeluca@unime.it (L.D. Luca).

0968-0896/$ - see front matter Crown Copyright © 2010 Published by Elsevier Ltd. All rights reserved.
doi:10.1016/j.bmc.2010.06.063

Unfortunately, a full understanding of the binding mode of INSTIs has been hampered by the lack of detailed information about the structure of the three-domain protein and its interaction with the DNA substrates (viral and target DNA), metal cofactors and inhibitors. In the last decade of antiviral research, the discovery of the keto-enol acid class, often referred as diketoacid (DKA) class, and their analogues and bioisosters as IN inhibitors was a major advance in the validation of IN as a therapeutically viable antiretroviral drug target.[12,14–18]

In particular a DKA-analogue MK-0518 (**1**), known as raltegravir, is the first and only integrase inhibitor (INI) approved by the Food and Drug Administration (FDA) for the treatment of AIDS acting as INSTI.[19–21]

Moreover other HIV-1 IN inhibitors that have been clinically evaluated, such as GS-9137 (**2**), MK-2048 (**3**), GS-9160, GS-9224, GSK-364735, and BMS-707035 belong to the same chemical class of DKA-like derivatives which have been shown to specifically inhibit the DNA ST step of integration and represent the major leads in the development of anti-HIV-1 IN drugs.[22]

Previously, our molecular modeling studies had suggested to us the rational design and synthesis of new potential DKA-INIs characterized by the presence of a 1*H*-benzylindole skeleton.[23,24] The biological results showed that all derivatives selectively inhibited the ST step at nanomolar concentration and in particular allowed us to identify a new 'lead compound' named CHI-1043 (**4**) characterized by the presence of a methoxy group at C-4 of the indole system and bearing a fluorine atom on the para position of the benzyl moiety (Fig. 1).[25]

On these bases, and also taking into account some structural characteristics of potent IN inhibitors in clinical trials (i.e., GS-9137 elvitegravir (**2**), MK-2048 (**3**) etc.) we herein report the rational design, synthesis and structure–activity relationships (SAR) of new chloro–fluoro-benzylindoles CHI-1043 analogues with the aim of improving the activity of this class of compounds as well as their selective index. Finally, docking results are herein reported to further clarify their mechanism of action.

2. Results and discussion

2.1. Rational design

The IN strand-transfer reaction occurs inside the nucleus and produces a functional integrated proviral DNA which forms the template for transcription of new viral RNA needed for new virions.[26] Thus without successful integration, viral replication would stall leading to a rapid decline in the viral load and then of the infection. For these reason, intensive research over the last two decades have been addressed to the discovery and development of small molecules inhibitors of the INST. Several previous publications have described our intense work on anti-HIV agents.[23,24,27–34] In particular, we generated a 3D pharmacophore model by Catalyst program for DKA-like derivatives acting as INSTIs[25] consisting of seven features: four hydrogen-bond acceptors (A1–A4), two hydrophobic aliphatic regions (Z1 and Z2) and one aromatic feature (Y). The superimposition of our lead compound CHI-1043 on the model is shown in Figure 2A: the β-diketo acid moiety maps the three hydrogen-bond acceptors (A1–A3), the methoxy group occupies aliphatic region Z1 and the *p*-fluorobenzyl ring overlaps the aromatic feature Y. For the purpose of lead optimization, the effect of introducing substituents on the benzene-fused ring of an indole system has already been examined[25] and the biological results showed that the methoxy derivatives exhibited the best biological profile inhibiting HIV-1 IN at a nanomolar to low micromolar range. Encouraged by these results and in order to extend our understanding of the structure–activity relationships of this class of INIs and explore the chemical features required for the IN inhibition, we decided to keep unchanged the indole part of the molecule and to investigate the effects of different substituents on the benzyl group at N1.

Although INSTIs are structurally diverse and encompass a variety of pharmacophores, all appear to have features in common, reflecting a likely similar mode of action. In particular, the presence of a metal-binding moiety, in our compounds represented by the hydroxy acid group, and an enzyme-binding moiety appears specially important. This last portion contains one or more aromatic hydrophobic residues needed to anchor the INSTIs to a hydrophobic pocket that forms upon binding of viral DNA.[35] In particular a halogen-substituted aromatic functionality linked to the chelating portion of the inhibitors has been hypothesized may bind in one or more hydrophobic pockets of IN–DNA complex.

Furthermore, several reports highlighted the importance of the halogen substituents effects on IN inhibitory potency. In particular we observed that some new HIV-1 IN inhibitors in clinical phase, including compounds such as elvitegravir (**2**) and MK-2048 (**3**), were charactherized by a chloro,fluorobenzyl substitution as common feature.

The superimposition of these compounds on our pharmacophore hypothesis showed that the chloro,fluorobenzyl moiety of these ligands occupied the hydrophobic feature Y of our model (Fig. 2B–C). This observation suggested to us some chemical mod-

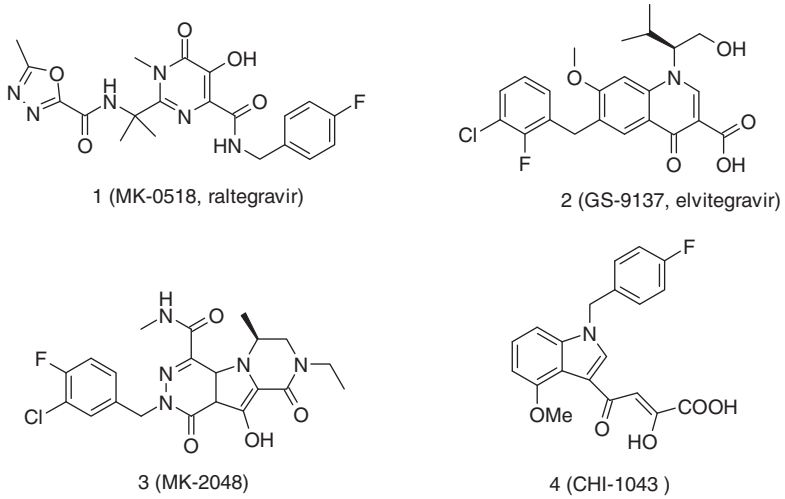

Figure 1. Chemical structures of integrase strand-transfer inhibitors.

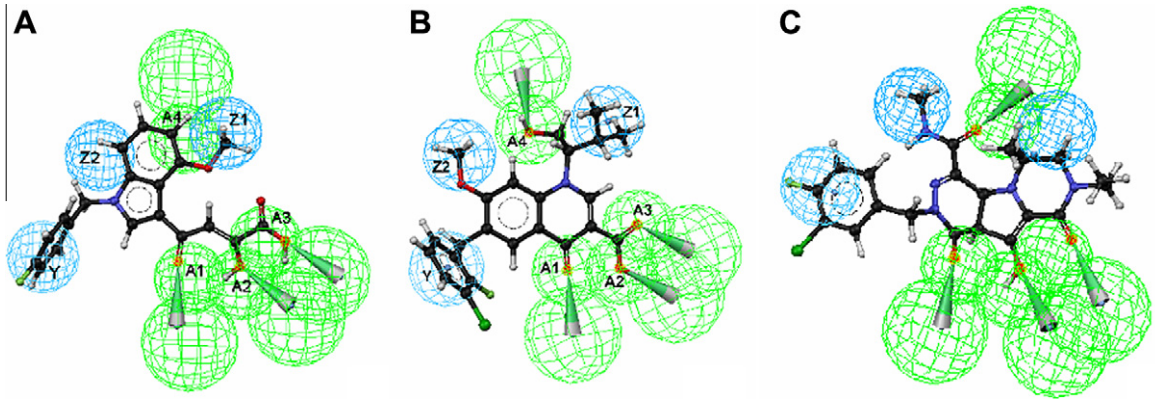

Figure 2. The top scoring HipHop pharmacophore Hypo1 is mapped to IN inhibitors 4 (A), **2** (B) **3** (C) (A1–A4, hydrogen-bond acceptor, green; Z1–Z2, hydrophobic aliphatic, blue; Y, hydrophobic aromatic, cyan).

ifications on this part of our lead compound CHI-1043. With the aim of studying the effect on biological activity of the nature and position of substituents on the benzyl moiety we replaced the fluoro to chloro group and also examined the influence of introducing two or more substituents in different positions.

A small library of novel chloro,fluorobenzyl derivatives (**20–45**) was then designed and tested as INIs and anti-HIV agents (see Sections 2.2 and 2.3).

2.2. Chemistry

With the aim of obtaining further information about the structure–activity relationship (SAR) of the benzylindole DKA derivatives **20–45** we planned the synthesis of the designed compounds.

Previously[25,36] we described the preparation of 4-[1-benzyl-4-methoxy-1*H*-indol-3-yl]-2-hydroxy-4-oxobut-2-enoic acids in which several steps of the synthetic approach were optimized by the application of microwave-assisted technology, thereby increasing the yields and reducing the reaction times as well as having cleaner reactions and using less solvent.

We report herein an alternative way to perform the 3-acetylation of 4-OCH_3-1*H*-indole (**5**) through a similar Vilsmeier–Haack reaction using *N*,*N*-dimethylacetamide and phosphoryl chloride according to the procedure reported by Murakami et al.[37] This approach led to a significant improvement in reaction conditions giving a cleaner reaction and increasing the yield of the intermediate **6**. (Scheme 1).

Successively, by application of microwave assisted synthesis it was N-alkylated by treatment with the appropriate substituted-benzyl bromide to give intermediates **7–19**.

Coupling with diethyl oxalate easily provided diketo esters **20–32** which were finally converted into the corresponding benzylindolediketo acids (**33–45**) in basic medium.

The structural characteristics of obtained compounds were determined by means of analytic and spectroscopic methods.

2.3. Biological activity

All the synthesized derivatives, diketo esters (**20–32**) and the corresponding diketo acids (**33–45**), which were designed to merge their features with those of our previously reported benzylindole derivatives (i.e., CHI-1043), were tested. Their inhibitory effect on IN enzymatic activity and against HIV-1 replication (Table 1) was compared with those of some our already published substituted fluorobenzyl derivatives.[36]

To determine the susceptibility of the HIV-1 integrase enzyme towards synthesized compounds we used enzyme-linked immunosorbent assays as described previously.[38] However, their inhibitory effect on the HIV-induced cytopathic effect (CPE) in human lymphocyte MT-4 cell culture was determined by the MT-4/MTT-assay.[39]

Also in this new series of molecules the diketo acids (**33–35** and **37–45**) inhibited the enzyme at nanomolar concentration and exhibit a higher potency than that of the corresponding esters (**20–22**) and (**24–32**), thus suggesting the importance of ionizable carboxylic acid as metal ion binding motif. Surprendently derivative **36**, showed a different behavior limitedly to the enzymatic activity.

The biological results suggested that compounds bearing only a chlorine atom on 2- (**33**) or 3-position (**34**) were more potent than 4-substituted derivative (**35**) at inhibiting both over-all and strand-transfer steps as well as HIV replication in MT-4 cells.

Moreover, out of the disubstituted derivatives, compounds **37–43** showed a potent inhibition of strand-transfer and in over-all steps thus indicating the importance to maintain a chloro substitution at 2- or 3-position of the benzyl moiety. Moreover derivative **39** with the chloro substituent at the C-2 and a fluoro group at C-6 displayed a good antiviral activity and the highest selectivity index in the current series of molecules (Table 1).

With these findings our study may contribute to extend the understanding of the structure–activity parameters proving that the diversity of halogen-substituted benzyl groups influences the inhibition potency and the selectivity of these INIs.

2.4. Molecular modeling studies

In order to better analyze their possible accommodation into the active site, we also performed docking studies on this new series of compounds starting from our previous results which provided new insights into the possible mechanism of action and binding mode of INSTIs.[40]

In particular, a ternary HIV-1 IN–Mg–DNA model was built and used by us as target for induced-fit docking (IFD) studies. Our in silico results were consistent with the available resistance mutation data and revealed that all the inhibitors bound the same region of the protein and share a similar mode of action at the IN active site. More specifically, the compounds: (a) have a pharmacophore that can establish interactions with the Mg^{2+} ions; (b) showed close interactions with the three catalytic residues (D64, D116 and E152); (c) interacted with the viral donor DNA and (d) were able to occupy a deep region defined by the catalytic loop and the viral DNA through their substituted aromatic tail.

The same IFD protocol has now been applied to the most active compounds herein reported in order to explore their possible binding conformation.

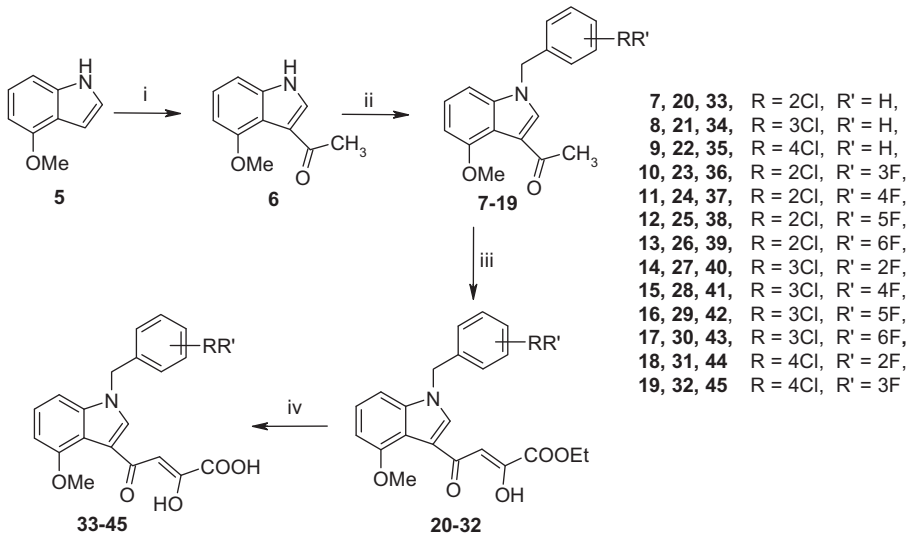

Scheme 1. Reagents and conditions: (i) $POCl_3$, $CH_3CON(CH_3)_2$, rt,12 h; (ii) $ArCH_2Br$, NaH, DMF, 50 °C, 5 min, 100 Watt; (iii) diethyl oxalate, dry CH_3ONa, THF, two separate steps under the same conditions: 50 °C, 2 min, 250 Watt; (iv) 2 N NaOH, MeOH, rt, 1.5 h.

Table 1
Inhibition of HIV-1 integrase enzymatic activity, replication of HIV-1 (IIIB), and cytotoxicity in MT-4 cells

Compound	IN enzymatic activity		Activity in MT-4 cells		
	Over-all[a] IC_{50} (μM)	ST[b] IC_{50} (μM)	HIV-1[c] EC_{50} (μM)	Cytotoxicity[d] EC_{50} (μM)	SI[e]
20	13.1 ± 0.4	0.73 ± 0.18	2.51 ± 0.08	34.51 ± 4.64	14
21	4.78 ± 1.56	2.89 ± 0.86	3.25 ± 0.86	52.89 ± 3.76	17
22	5.78 ± 3.85	8.26 ± 4.32	41.32 ± 0.00	41.32 ± 0.00	1
23	1.39 ± 0.78	9.2 ± 6.79	2.52 ± 0.26	18.5 ± 3.5	7
24	1.74 ± 0.79	2.56 ± 1.17	4.06 ± 1.56	51.43 ± 28.35	13
25	2.7 ± 0.25	2.94 ± 1.88	16.39 ± 0.6	39.63 ± 5.67	3
26	2.86 ± 1.07	1.2 ± 0.11	4.66 ± 0.00	25.36 ± 0.00	5
27	1.37 ± 0.14	0.74 ± 0.26	2.31 ± 0.02	46.9 ± 0.00	20
28	0.36 ± 0.1	0.07 ± 0.04	1.87 ± 0.19	49.3 ± 3.6	26
29	1.30 ± 0.09	3.17 ± 0.70	4.27 ± 0.68	58.2 ± 3.9	14
30	1.61 ± 1.37	0.89 ± 0.53	18.13 ± 0.00	18.13 ± 0.00	1
31	1.15 ± 0.22	3.32 ± 1.31	>17.00	17.00 ± 0.00	<1
32	5.05 ± 2.62	20.35 ± 5.52	>63.68	63.70	<1
33	0.71 ± 0.24	0.52 ± 0.35	0.42 ± 0.00	27.0	64
34	0.13 ± 0.09	0.03 ± 0.01	0.64 ± 0.00	30.15 ± 1.85	47
35	1.02 ± 0.94	0.59 ± 0.06	20.58 ± 0.00	33.47 ± 5.27	2
36	5.24 ± 1.23	12.74 ± 1.79	0.36 ± 0.05	6.5 ± 0.5	18
37	0.54 ± 0.14	0.06 ± 0.04	4.3 ± 2.1	47.16 ± 4.9	11
38	0.42 ± 0.16	0.27 ± 0.07	3.3 ± 0.86	26.26 ± 4.13	8
39	0.53 ± 0.38	0.13 ± 0.03	0.56 ± 0.003	61.97 ± 22.84	111
40	0.74 ± 0.21	0.03 ± 0.02	0.43 ± 0.00	14.95 ± 3.65	35
41	0.04 ± 0.00	0.12 ± 0.01	0.43 ± 0.005	31.65 ± 18.25	74
42	0.24 ± 0.01	0.25 ± 0.01	0.52 ± 0.05	32.15 ± 3.05	62
43	0.32 ± 0.08	0.09 ± 0.02	4.17	10.75 ± 2.95	3
44	2.53 ± 0.39	5.52 ± 1.58	>22.52	23.00 ± 0.5	<1
45	3.33 ± 0.89	4.58 ± 0.19	>23.31	23.31	<1
CHI-1043	0.08 ± 0.003	0.14 ± 0.11	0.59 ± 0.38	41.1 ± 16.7	70
MK-518	0.009 ± 0.0002	0.007 ± 0.0005	0.013 ± 0.0005	>18	>1387
GS-9137	0.004 ± 0.003	0.015 ± 0.002	0.0008 ± 0.00009	2.12 ± 0.36	>2650

[a] Concentration required to inhibit the in vitro overall integrase activity by 50%.
[b] Concentration required to inhibit the in vitro strand-transfer step by 50%.
[c] Effective concentration required to reduce HIV-1-induced cytopathic effect by 50% in MT-4 cells.
[d] Cytotoxic concentration to reduce MT-4 cell viability by 50%.
[e] Selectivity index: ratio CC_{50}/EC_{50}. All data represent average results ± SD.

Figure 3 reports the binding mode of derivative **39**, selected for its interesting biological profile (Table 1): it is active at nanomolar concentration as INST inhibitor and shows potent antiviral activity against HIV-1 in MT-4 cells as well as the highest selectivity index of the series.

The results of the IFD study showed that compound **39** is able to interact with the Mg^{2+} ions and also presents close interactions with both viral DNA strands (Fig. 3).

The benzyl group points toward the active site loop (residues 140–149), making strong hydrophobic interactions with I141; no

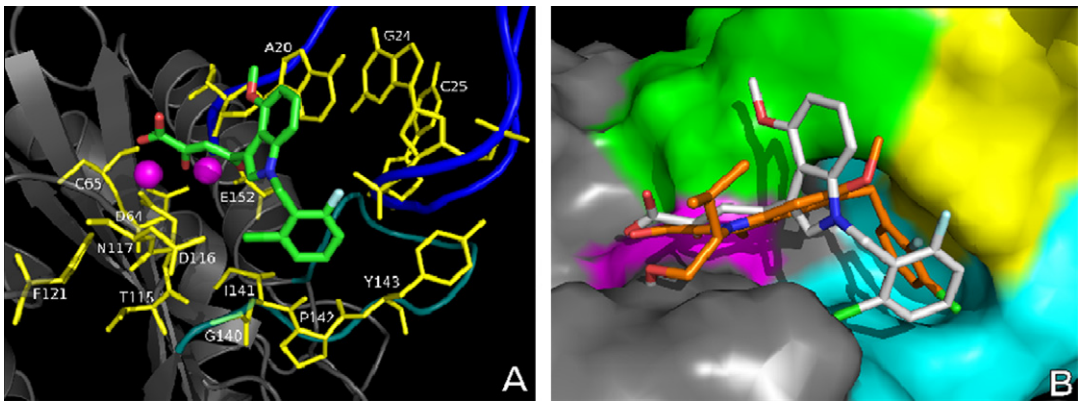

Figure 3. (A) Induced-fit docking results for 39. IN/DNA residues lying within a distance of 5 Å from the docked inhibitor are shown in yellow. G24 and C25 are 5′-DNA nucleotide bases, while A20 is the terminal adenine of the 3′-processed viral DNA. The divalent metal ions are shown as magenta spheres, the active site loop is highlighted in cyan, and the viral DNA backbone is depicted in blue. B) Binding mode for 39. Molecular surfaces are shown for IN (gray), catalytic loop (residues 140–149; cyan), metal ions (magenta), 3′-DNA strand (green), and 5′-DNA strand (yellow). IFD conformations for 39 and elvitegravir (2) are colored in white and orange, respectively. This figure was prepared using PyMol.[46]

hydrogen-bond was observed between our compound and the macromolecular target (Fig. 3A). A comparison between the IFD conformations obtained for elvitegravir (**2**) and compound **39** highlighted that their substituted aromatic tail occupy a similar region of the macromolecular target: the fluoro,chlorobenzyl group of both molecules was in fact directed toward the active site loop residues and deeply occupies a region defined by the loop itself and the donor DNA (Fig. 3B).

3. Conclusion

We herein report design, synthesis and biological evaluation of a new series of potent INIs which allowed us to further clarify the SAR of our benzylindolediketo acids. In this study we extended the investigation of the hydrophobic portion that is of the enzyme-binding moiety of INSTIs. As a result some new derivatives more potent and with a selectivity index higher than that of our lead compound CHI-1043 were obtained. In some cases the new molecules (**34**, **37** and **40**), showed an IN strand-transfer inhibition comparable to that of elvitegravir (**2**).

Finally, the IFD results highlighted that our derivatives present a binding mode similar to that of elvitegravir (**2**) and confirmed the importance of lipophilic groups able to occupy the hydrophobic cavity in the INSTI binding site. Considering that the diketo acid moiety seems to negatively influence the selectivity of the molecules, additional modifications in this direction are in progress to further optimize the biological profile of so far obtained compounds and in an attempt to throw useful structural information to construct ideal INSTIs.

4. Experimental section

4.1. Preparation of IN–DNA–Mg complex and ligands for the IFD protocol

Ligand structures were constructed using the Schrçdinger Maestro[41] and were then submitted to Polak–Ribiere conjugate gradient minimization (0.0005 kJÅ^{-1} mol^{-1} convergence). The compounds were presented in their enolic tautomeric form, since it has been clearly established that DKAs mainly exist in this form in solution, the carboxylic moiety was considered as carboxylate, and the enolic oxygen was considered as enolate given the influence of the two metal ions in the binding site.[42]

4.2. Induced-fit methodology

The IFD protocol[43] developed by Schrçdinger[44] was employed in this study. Briefly, IFD methodology uses the docking program Glide to account for ligand flexibility and the Refinement module in the Prime program to account for receptor flexibility. The Schrçdinger IFD protocol models induced-fit docking of one or more ligands using the following steps (the description below is from the IFD manual):

1. Constrained minimization of the receptor (Glide protein preparation, refinement only) with an RMSD cutoff of 0.18.
2. Initial Glide docking of each ligand using a softened potential (van der Waals radii scaling). By default, a maximum 20 poses per ligand are retained, and by default, poses to be retained must have a Coulomb–vdW score <100 and an H-bond score <−0.05.
3. One round of Prime side chain prediction for each protein–ligand complex, on residues within a given distance of any ligand pose (6 Å in our study).
4. Prime minimization of the same set of residues and the ligand for each protein–ligand complex pose. The receptor structure in each pose now reflects an induced-fit to the ligand structure and conformation.
5. Glide re-docking of each protein–ligand complex structure within a specified energy of the lowest-energy structure (default: 30 kcalmol −1). The ligand is now rigorously docked, using default Glide settings, into the induced-fit receptor structure.
6. Estimation of the binding energy (IFDScore) for each output pose.

In our study, all docking calculations were run in the ‘Standard Precision’ mode of Glide, and the center of the grid box was defined by the manually selected Mg ions. All of the docked structures were automatically ranked according to the IFD score. RMSDs were computed by all atoms except non polar hydrogen atoms.

4.3. Chemistry

All microwave-assisted reactions were carried out in a CEM Focused Microwave Synthesis System, Model Discover working at the potency necessary for refluxing under atmospheric conditions (i.e., 250–300 W). Melting points were determined on a BUCHI Melting

Point B-545 apparatus and are uncorrected. Elemental analyses (C, H and N) were carried out on a Carlo Erba Model 1106 Elemental Analyzer and the results are within ±0.4% of the theoretical values. Merck Silica Gel 60 F254 plates were used for analytical TLC; column chromatography was performed on Merck silica gel 60 (230–400 mesh) and Flash Chromatography (FC) on a Biotage SP1 EXP. ^{1}H NMR spectra were recorded in $CDCl_3$ with TMS as internal standard or DMSO on a Varian Gemini-300 spectrometer. Chemical shifts are expressed in δ (ppm) and coupling constants (J) in hertz.

4.3.1. Synthesis of 3-acetyl-4-methoxy-1*H*-indole (6)

Phosphoryl chloride (0.92 ml, 10 mmol) was added to ice cold dimethylacetamide (2.79 ml, 30 mmol) with stirring and cooling in ice. 4-Methoxy-1*H*-indole 5 (147.18 mg, 1 mmol) was added and reaction mixture was stirred at room temperature for 12 h, then poured over ice and basified with 4 N aqueous sodium hydroxide solution. The mixture was extracted with ethyl acetate and dried over Na_2SO_4. After removal of the solvent under reduced pressure, the residue was powdered by treatment with diethyl ether and recrystallized from dichloromethane. Mp 113–115 °C, yield 89%. ^{1}H NMR (δ) 2.70 (s, 3H, CH_3), 3.97 (s, 3H, OCH_3), 6.68–7.79 (m, 4H, ArH), 8.69 (br s, 1H, NH). Anal. Calcd for $C_{11}H_{11}NO_2$: C, 69.83; H, 5.86; N, 7.40. Found: C, 69.62; H, 5.63; N, 7.51.

3-Acetyl-4-methoxy-1-benzyl-1*H*-indoles (**7–19**) were prepared following previously reported procedure.[36]

4.3.2. 3-Acetyl-1-(2-chlorobenzyl)-4-methoxy-1*H*-indole (7)

Mp 131–133 °C, yield 40%; ^{1}H NMR δ 2.50 (s, 3H, CH_3), 3.87 (s, 3H, OCH_3), 5.54 (s, 2H, CH_2), 6.72–8.07 (m, 8H, ArH). Anal. Calcd for $C_{18}H_{16}ClNO_2$: C, 68.90; H, 5.14; N, 4.46. Found: C, 69.07; H, 5.34; N, 4.13.

4.3.3. 3-Acetyl-1-(3-chlorobenzyl)-4-methoxy-1*H*-indole (8)

Mp 115–117 °C, yield 63%;^{1}H NMR (δ) 2.62 (s, 3H, CH_3), 3.94 (s, 3H, OCH_3), 5.37 (s, 2H, CH_2), 6.69–7.84 (m, 8H, ArH). Anal. Calcd for $C_{18}H_{16}ClNO_2$: C, 68.90; H, 5.14; N, 4.46. Found: C, 68.72; H, 5.42; N, 4.64.

4.3.4. 3-Acetyl-1-(4-chlorobenzyl)-4-methoxy-1*H*-indole (9)

Mp 129–131 °C, yield 60%; ^{1}H NMR (δ) 2.53 (s, 3H, CH_3), 3.84 (s, 3H, OCH_3), 5.44 (s, 2H, CH_2), 6.69–8.19 (m, 8H, ArH). Anal. Calcd for $C_{18}H_{15}Cl_2NO_2$: C, 68.90; H, 5.14; N, 4.46. Found: C, 69.12; H, 5.06; N, 4.24.

4.3.5. 3-Acetyl-1-(2-chloro-3-fluorobenzyl)-4-methoxy-1*H*-indole (10)

Mp 165–167 °C, yield 68%; ^{1}H NMR (δ) 2.70 (s, 3H, CH_3), 3.99 (s, 3H, OCH_3), 5.41 (s, 2H, CH_2), 6.46–7.71 (m, 7H, ArH). Anal. Calcd for $C_{18}H_{15}ClFNO_2$: C, 65.16; H, 4.56; N, 4.22. Found: C, 65.32; H, 4.28; N, 4.06.

4.3.6. 3-Acetyl-1-(2-chloro-4-fluorobenzyl)-4-methoxy-1*H*-indole (11)

Mp 151–153 °C, yield 67%; ^{1}H NMR (δ) 2.70 (s, 3H, CH_3), 3.99 (s, 3H, OCH_3), 5.35 (s, 2H, CH_2), 6.67–7.70 (m, 7H, ArH). Anal. Calcd for $C_{18}H_{15}ClFNO_2$: C, 65.16; H, 4.56; N, 4.22. Found: C, 65.42; H, 4.37; N, 4.31.

4.3.7. 3-Acetyl-1-(2-chloro-5-fluorobenzyl)-4-methoxy-1*H*-indole (12)

Mp 132–134 °C, yield 42%; ^{1}H NMR (δ) 2.54 (s, 3H, CH_3), 3.87 (s, 3H, OCH_3), 5.53 (s, 2H, CH_2), 6.52–8.09 (m, 7H, ArH). Anal. Calcd for $C_{18}H_{15}ClFNO_2$: C, 65.16; H, 4.56; N, 4.22. Found: C, 65.27; H, 4.73; N, 4.08.

4.3.8. 3-Acetyl-1-(2-chloro-6-fluorobenzyl)-4-methoxy-1*H*-indole (13)

Mp 108–110 °C, yield 46%; ^{1}H NMR (δ) 2.65 (s, 3H, CH_3), 3.96 (s, 3H, OCH_3), 5.41 (s, 2H, CH_2), 6.69–7.67 (m, 7H, ArH). Anal. Calcd for $C_{18}H_{15}ClFNO_2$: C, 65.16; H, 4.56; N, 4.22. Found: C, 65.02; H, 4.64; N, 4.35.

4.3.9. 3-Acetyl-1-(3-chloro-2-fluorobenzyl)-4-methoxy-1*H*-indole (14)

Mp 121–123 °C, yield 71%; ^{1}H NMR (δ) 2.70 (s, 3H, CH_3), 3.98 (s, 3H, OCH_3), 5.36 (s, 2H, CH_2), 6.69–7.75 (m, 7H, ArH). Anal. Calcd for $C_{18}H_{15}ClFNO_2$: C, 65.16; H, 4.56; N, 4.22. Found: C, 65.23; H, 4.71; N, 4.11.

4.3.10. 3-Acetyl-1-(3-chloro-4-fluorobenzyl)-4-methoxy-1*H*-indole (15)

Mp 103–105 °C, yield 61%; ^{1}H NMR (δ) 2.70 (s, 3H, CH_3), 3.97 (s, 3H, OCH_3), 5.24 (s, 2H, CH_2), 6.69–7.71 (m, 7H, ArH). Anal. Calcd for $C_{18}H_{15}ClFNO_2$: C, 65.16; H, 4.56; N, 4.22. Found: C, 65.02; H, 4.44; N, 4.57.

4.3.11. 3-Acetyl-1-(3-chloro-5-fluorobenzyl)-4-methoxy-1*H*-indole (16)

Mp 133–135 °C, yield 66%; ^{1}H NMR (δ) 2.71 (s, 3H, CH_3), 3.98 (s, 3H, OCH_3), 5.26 (s, 2H, CH_2), 6.69–7.71 (m, 7H, ArH). Anal. Calcd for $C_{18}H_{15}ClFNO_2$: C, 65.16; H, 4.56; N, 4.22. Found: C, 65.27; H, 4.71; N, 4.09.

4.3.12. 3-Acetyl-1-(3-chloro-6-fluorobenzyl)-4-methoxy-1*H*-indole (17)

Mp 123–125 °C, yield 68%; ^{1}H NMR (δ) 2.70 (s, 3H, CH_3), 3.98 (s, 3H, OCH_3), 5.30 (s, 2H, CH_2), 6.70–7.74 (m, 7H, ArH). Anal. Calcd for $C_{18}H_{15}ClFNO_2$: C, 65.16; H, 4.56; N, 4.22. Found: C, 65.33; H, 4.62; N, 4.13.

4.3.13. 3-Acetyl-1-(4-chloro-2-fluorobenzyl)-4-methoxy-1*H*-indole (18)

Mp 140–142 °C, yield 66%; ^{1}H NMR (δ) 2.69 (s, 3H, CH_3), 3.97 (s, 3H, OCH_3), 5.30 (s, 2H, CH_2), 6.68–7.72 (m, 7H, ArH). Anal. Calcd for $C_{18}H_{15}ClFNO_2$: C, 65.16; H, 4.56; N, 4.22. Found: C, 65.38; H, 4.27; N, 4.51.

4.3.14. 3-Acetyl-1-(4-chloro-3-fluorobenzyl)-4-methoxy-1*H*-indole (19)

Mp 158–160, yield 72%; ^{1}NMR (δ) 2.71 (s, 3H, CH_3), 3.98 (s, 3H, OCH_3), 5.27 (s, 2H, CH_2), 6.69–7.71 (m, 7H, ArH). Anal. Calcd for $C_{18}H_{15}ClFNO_2$: C, 65.16; H, 4.56; N, 4.22. Found: C, 65.32; H, 4.24; N, 4.31.

Ethyl 4-[1-benzyl-4-methoxy-1*H*-indol-3-yl]-2-hydroxy-4-oxo-but-2-enoates (**20–32**) were prepared following previously reported procedure.[36]

4.3.15. Ethyl 4-[1-(2-chlorobenzyl)-4-methoxy-1*H*-indol-3-yl]-2-hydroxy-4-oxobut-2-enoate (20)

Mp 205 °C dec, yield 93%; ^{1}H NMR (δ) 1.23 (t, J = 7.1, 3H, CH_3), 3.84 (s, 3H, OCH_3), 4.10 (q, J = 7.1, 2H, CH_2), 5.47 (s, 2H, CH_2), 6.56–8.52 (m, 9H, 8ArH and CH). Anal. Calcd for $C_{22}H_{20}ClNO_5$: C, 63.85; H, 4.87; N, 3.38. Found: C, 63.56; H, 4.41; N, 3.52.

4.3.16. Ethyl 4-[1-(3-chlorobenzyl)-4-methoxy-1*H*-indol-3-yl]-2-hydroxy-4-oxobut-2-enoate (21)

Mp 180 °C dec, yield 87%; ^{1}H NMR (δ) 1.23 (t, J = 7.1, 3H, CH_3), 3.82 (s, 3H, OCH_3), 4.10 (q, J = 7.1, 2H, CH_2), 5.41 (s, 2H, CH_2), 6.56–8.51 (m, 9H, 8ArH and CH). Anal. Calcd for $C_{22}H_{20}ClNO_5$: C, 63.85; H, 4.87; N, 3.38. Found: C, 63.71; H, 4.94 N, 3.25.

4.3.17. Ethyl 4-[1-(4-chlorobenzyl)-4-methoxy-1*H*-indol-3-yl]-2-hydroxy-4-oxobut-2-enoate (22)

Mp 215 °C dec, yield 91%; ^{1}H NMR (δ) 1.22 (t, J = 7.1, 3H, CH_3), 3.82 (s, 3H, OCH_3), 4.10 (q, J = 7.1, 2H, CH_2), 5.39 (s, 2H, CH_2), 6.55–8.51 (m, 9H, 8ArH and CH). Anal. Calcd for $C_{22}H_{20}ClNO_5$: C, 63.85; H, 4.87; N, 3.38. Found: C, 63.61; H, 4.95 N, 3.54.

4.3.18. Ethyl 4-[1-(2-chloro-3-fluorobenzyl)-4-methoxy-1*H*-indol-3-yl]-2-hydroxy-4-oxobut-2-enoate (23)

Mp 242 °C dec, yield 96%; ^{1}H NMR (δ) 1.22 (t, J = 7.1, 3H, CH_3), 3.84 (s, 3H, OCH_3), 4.09 (q, J = 7.1, 2H, CH_2), 5.53 (s, 2H, CH_2), 6.52–7.60 (m, 8H, 7ArH and CH). Anal. Calcd for $C_{22}H_{19}ClFNO_5$: C, 61.19; H, 4.43; N, 3.24. Found: C, 61.29; H, 4.63; N, 3.53.

4.3.19. Ethyl 4-[1-(2-chloro-4-fluorobenzyl)-4-methoxy-1*H*-indol-3-yl]-2-hydroxy-4-oxobut-2-enoate (24)

Mp 250 °C dec, yield 89%; ^{1}H NMR (δ) 1.22 (t, J = 7.1, 3H, CH_3), 3.83 (s, 3H, OCH_3), 4.08 (q, J = 7.1, 2H, CH_2), 5.44 (s, 2H, CH_2), 6.58–8.49 (m, 8H, 7ArH and CH). Anal. Calcd for $C_{22}H_{19}ClFNO_5$: C, 61.19; H, 4.43; N, 3.24. Found: C, 61.44; H, 4.72; N, 3.51.

4.3.20. Ethyl 4-[1-(2-chloro-5-fluorobenzyl)-4-methoxy-1*H*-indol-3-yl]-2-hydroxy-4-oxobut-2-enoate (25)

Mp 190 °C dec, yield 88%; ^{1}H NMR (δ) 1.23 (t, J = 7.1, 3H, CH_3), 3.84 (s, 3H, OCH_3), 4.10 (q, J = 7.1, 2H, CH_2), 5.47 (s, 2H, CH_2), 6.48–8.49 (m, 8H, 7ArH and CH). Anal. Calcd for $C_{22}H_{19}ClFNO_5$: C, 61.19; H, 4.43; N, 3.24. Found: C, 61.32; H, 4.26; N, 3.52.

4.3.21. Ethyl 4-[1-(2-chloro-6-fluorobenzyl)-4-methoxy-1*H*-indol-3-yl]-2-hydroxy-4-oxobut-2-enoate (26)

Mp 245 °C dec, yield 91%; ^{1}H NMR (δ) 1.22 (t, J = 7.1, 3H, CH_3), 3.83 (s, 3H, OCH_3), 4.10 (q, J = 7.1, 2H, CH_2), 5.46 (s, 2H, CH_2), 6.63–8.48 (m, 8H, 7ArH and CH). Anal. Calcd for $C_{22}H_{19}ClFNO_5$: C, 61.19; H, 4.43; N, 3.24. Found: C, 61.44; H, 4.72; N, 3.09.

4.3.22. Ethyl 4-[1-(3-chloro-2-fluorobenzyl)-4-methoxy-1*H*-indol-3-yl]-2-hydroxy-4-oxobut-2-enoate (27)

Mp 198–200 °C, yield 88%; ^{1}H NMR (δ) 1.23 (t, J = 7.1, 3H, CH_3), 3.81 (s, 3H, OCH_3), 4.11 (q, J = 7.1, 2H, CH_2), 5.41 (s, 2H, CH_2), 6.56–8.49 (m, 8H, 7ArH and CH). Anal. Calcd for $C_{22}H_{19}ClFNO_5$: C, 61.19; H, 4.43; N, 3.24. Found: C, 61.24; H, 4.56; N, 3.37.

4.3.23. Ethyl 4-[1-(3-chloro-4-fluorobenzyl)-4-methoxy-1*H*-indol-3-yl]-2-hydroxy-4-oxobut-2-enoate (28)

Mp 207 °C dec, yield 79%; ^{1}H NMR (δ) 1.22 (t, J = 7.1, 3H, CH_3), 3.81 (s, 3H, OCH_3), 4.08 (q, J = 7.1, 2H, CH_2), 5.38 (s, 2H, CH_2), 6.50–8.52 (m, 8H, 7ArH and CH). Anal. Calcd for $C_{22}H_{19}ClFNO_5$: C, 61.19; H, 4.43; N, 3.24. Found: C, 61.53; H, 4.62; N, 3.58.

4.3.24. Ethyl 4-[1-(3-chloro-5-fluorobenzyl)-4-methoxy-1*H*-indol-3-yl]-2-hydroxy-4-oxobut-2-enoate (29)

Mp 223–225 °C, yield 82%; ^{1}H NMR (δ) 1.21 (t, J = 7.1, 3H, CH_3), 3.81 (s, 3H, OCH_3), 4.12 (q, J = 7.1, 2H, CH_2), 5.41 (s, 2H, CH_2), 6.62–8.49 (m, 8H, 7ArH and CH). Anal. Calcd for $C_{22}H_{19}FNO_5$: C, 61.19; H, 4.43; N, 3.24. Found: C, 61.32; H, 4.28; N, 3.48.

4.3.25. Ethyl 4-[1-(3-chloro-6-fluorobenzyl)-4-methoxy-1*H*-indol-3-yl]-2-hydroxy-4-oxobut-2-enoate (30)

Mp 198–200 °C dec, yield 86%; ^{1}H NMR (δ) 1.59 (t, J = 7.1, 3H, CH_3), 3.82 (s, 3H, OCH_3), 4.09 (q, J = 7.1, 2H, CH_2), 5.43 (s, 2H, CH_2), 6.53–8.51 (m, 8H, 7ArH and CH). Anal. Calcd for $C_{22}H_{19}ClFNO_5$: C, 61.19; H, 4.43; N, 3.24. Found: C, 61.34; H, 4.27; N, 3.51.

4.3.26. Ethyl 4-[1-(4-chloro-2-fluorobenzyl)-4-methoxy-1*H*-indol-3-yl]-2-hydroxy-4-oxobut-2-enoate (31)

Mp 228–230 °C dec, yield 89%; ^{1}H NMR (δ) 1.28 (t, J = 7.1, 3H, CH_3), 3.89 (s, 3H, OCH_3), 4.23 (q, J = 7.1, 2H, CH_2), 5.53 (s, 2H, CH_2), 6.76–8.33 (m, 8H, 7ArH and CH). Anal. Calcd for $C_{22}H_{19}ClFNO_5$: C, 61.19; H, 4.43; N, 3.24. Found: C, 61.32; H, 4.68; N, 3.39.

4.3.27. Ethyl 4-[1-(4-chloro-3-fluorobenzyl)-4-methoxy-1*H*-indol-3-yl]-2-hydroxy-4-oxobut-2-enoate (32)

Mp 186–188 °C, yield 81%; ^{1}H NMR (δ) 1.22 (t, J = 7.1, 3H, CH_3), 3.82 (s, 3H, OCH_3), 4.09 (q, J = 7.1, 2H, CH_2), 5.41 (s, 2H, CH_2), 6.53–8.50 (m, 8H, 7ArH and CH). Anal. Calcd for $C_{22}H_{19}ClFNO_5$: C, 61.19; H, 4.43; N, 3.24. Found: C, 61.44; H, 4.28; N, 3.42.

4-[1-Benzyl-4-methoxy-1*H*-indol-3-yl]-2-hydroxy-4-oxobut-2-enoic acid (**33–45**) were prepared following previously reported procedure.[36]

4.3.28. 4-[1-(2-Chlorobenzyl)-4-methoxy-1*H*-indol-3-yl]-2-hydroxy-4-oxobut-2-enoic acid (33)

Mp 160–162 °C, yield 65%; ^{1}H NMR (δ) 3.91 (s, 3H, OCH_3), 5.60 (s, 2H, CH_2), 6.78–8.36 (m, 9H, 8ArH and CH). Anal. Calcd for $C_{20}H_{16}ClNO_5$: C, 62.27; H, 4.18; N, 3.63. Found: C, 62.48; H, 4.61; N, 3.31.

4.3.29. 4-[1-(3-Chlorobenzyl)-4-methoxy-1*H*-indol-3-yl]-2-hydroxy-4-oxobut-2-enoic acid (34)

Mp 160–162 °C, yield 65%; ^{1}H NMR (δ) 3.90 (s, 3H, OCH_3), 5.52 (s, 2H, CH_2), 6.79–8.56 (m, 9H, 8ArH and CH). Anal. Calcd for $C_{20}H_{16}ClNO_5$: C, 62.27; H, 4.18; N, 3.63. Found: C, 62.38; H, 4.29; N, 3.47.

4.3.30. 4-[1-(4-Chlorobenzyl)-4-methoxy-1*H*-indol-3-yl]-2-hydroxy-4-oxobut-2-enoic acid (35)

Mp 170–172 °C, yield 48%; ^{1}H NMR (δ) 3.89 (s, 3H, OCH_3), 5.51 (s, 2H, CH_2), 6.78–8.53 (m, 9H, 8ArH and CH). Anal. Calcd for $C_{20}H_{16}ClNO_5$: C, 62.27; H, 4.18; N, 3.63. Found: C, 62.41; H, 4.35; N, 3.44.

4.3.31. 4-[1-(2-Chloro-3-fluorobenzyl)-4-methoxy-1*H*-indol-3-yl]-2-hydroxy-4-oxobut-2-enoic acid (36)

Mp 160–162 °C, yield 35%; ^{1}H NMR (δ) 3.92 (s, 3H, OCH_3), 5.66 (s, 2H, CH_2), 6.56–8.42 (m, 8H, 7ArH and CH). Anal. Calcd for $C_{20}H_{15}ClFNO_5$: C, 59.49; H, 3.74; N, 3.47. Found: C, 59.38; H, 3.61; N, 3.55.

4.3.32. 4-[1-(2-Chloro-4-fluorobenzyl)-4-methoxy-1*H*-indol-3-yl]-2-hydroxy-4-oxobut-2-enoic acid (37)

Mp 266–288 °C dec, yield 58%; ^{1}H NMR (δ) 3.85 (s, 3H, OCH_3), 5.51 (s, 2H, CH_2), 6.69–8.05 (m, 8H, 7ArH and CH). Anal. Calcd for $C_{20}H_{15}ClFNO_5$: C, 59.49; H, 3.74; N, 3.47. Found: C, 59.76; H, 3.97; N, 3.58.

4.3.33. 4-[1-(2-Chloro-5-fluorobenzyl)-4-methoxy-1*H*-indol-3-yl]-2-hydroxy-4-oxobut-2-enoic acid (38)

Mp 164–166 °C, yield 41%; ^{1}H NMR (δ) 3.92 (s, 3H, OCH_3), 5.60 (s, 2H, CH_2), 6.64–8.40 (m, 8H, 7ArH and CH). Anal. Calcd for $C_{20}H_{15}ClFNO_5$: C, 59.49; H, 3.74; N, 3.47. Found: C, 59.21; H, 3.59; N, 3.62.

4.3.34. 4-[1-(2-Chloro-6-fluorobenzyl)-4-methoxy-1*H*-indol-3-yl]-2-hydroxy-4-oxobut-2-enoic acid (39)

Mp 198–200 °C, yield 59%; ^{1}H NMR (δ) 3.90 (s, 3H, OCH_3), 5.62 (s, 2H, CH_2), 6.81–8.13 (m, 8H, 7ArH and CH). Anal. Calcd for $C_{20}H_{15}ClFNO_5$: C, 59.49; H, 3.74; N, 3.47. Found: C, 59.36; H, 3.61; N, 3.58.

4.3.35. 4-[1-(3-Chloro-2-fluorobenzyl)-4-methoxy-1*H*-indol-3-yl]-2-hydroxy-4-oxobut-2-enoic acid (40)

Mp 268 °C dec, yield 63%; ^{1}H NMR (δ) 3.85 (s, 3H, OCH_3), 5.57 (s, 2H, CH_2), 6.70–8.14 (m, 8H, 7ArH and CH). Anal. Calcd for $C_{20}H_{15}ClFNO_5$: C, 59.49; H, 3.74; N, 3.47. Found: C, 59.58; H, 3.52; N, 3.71.

4.3.36. 4-[1-(3-Chloro-4-fluorobenzyl)-4-methoxy-1*H*-indol-3-yl]-2-hydroxy-4-oxobut-2-enoic acid (41)

Mp 218–220 °C dec, yield 79%;^{1}H NMR (δ) 3.89 (s, 3H, OCH_3), 5.50 (s, 2H, CH_2), 6.78–8.55 (m, 8H, 7ArH and CH). Anal. Calcd for $C_{20}H_{15}ClFNO_5$: C, 59.49; H, 3.74; N, 3.47. Found: C, 59.61; H, 3.59; N, 3.31.

4.3.37. 4-[1-(3-Chloro-5-fluorobenzyl)-4-methoxy-1*H*-indol-3-yl]-2-hydroxy-4-oxobut-2-enoic acid (42)

Mp 165–167 °C, yield 71%; ^{1}H NMR (δ) 3.89 (s, 3H, OCH_3), 5.52 (s, 2H, CH_2), 6.81–8.56 (m, 8H, 7ArH and CH). $C_{20}H_{15}ClFNO_5$: C, 59.49; H, 3.74; N, 3.47. Found: C, 59.35; H, 3.51; N, 3.63.

4.3.38. 4-[1-(3-Chloro-6-fluorobenzyl)-4-methoxy-1*H*-indol-3-yl]-2-hydroxy-4-oxobut-2-enoic acid (43)

Mp 200–202 °C, yield 67%; ^{1}H NMR (δ) 3.84 (s, 3H, OCH_3), 5.49 (s, 2H, CH_2), 6.69–8.14 (m, 8H, 7ArH and CH). Anal. Calcd for $C_{20}H_{15}ClFNO_5$: C, 59.49; H, 3.74; N, 3.47. Found: C, 59.38; H, 3.43; N, 3.51.

4.3.39. 4-[1-(4-Chloro-2-fluorobenzyl)-4-methoxy-1*H*-indol-3-yl]-2-hydroxy-4-oxobut-2-enoic acid (44)

Mp 168–170 °C dec, yield 72%; ^{1}H NMR (δ) 3.90 (s, 3H, OCH_3), 5.57 (s, 2H, CH_2), 6.80–8.44 (m, 8H, 7ArH and CH). Anal. Calcd for $C_{20}H_{15}ClFNO_5$: C, 59.49; H, 3.74; N, 3.47. Found: C, 59.72; H, 3.68; N, 3.59.

4.3.40. 4-[1-(4-Chloro-3-fluorobenzyl)-4-methoxy-1*H*-indol-3-yl]-2-hydroxy-4-oxobut-2-enoic acid (45)

Mp 156–158 °C, yield 68%; ^{1}H NMR (δ) 3.90 (s, 3H, OCH_3), 5.53 (s, 2H, CH_2), 6.79–8.56 (m, 7H, 6ArH and CH). Anal. Calcd for $C_{20}H_{15}ClFNO_5$: C, 59.49; H, 3.74; N, 3.47. Found: C, 59.33; H, 3.62; N, 3.71.

4.3.41. Overall integrase assay using an enzyme-linked immunosorbent assay (ELISA)

To determine the susceptibility of the HIV-1 integrase enzyme towards different compounds we used enzyme-linked immunosorbent assays. These assays use an oligonucleotide substrate of which one oligonucleotide (5′-ACTGCTAGAGATTTTCCACACTGACT AAAAGGGTC-3′) is labeled with biotin at the 3′ end and the other oligonucleotide is labeled with digoxigenin at the 5′ end. For the overall integration assay the second 5′-digoxigenin labeled oligonucleotide is (5′-GACCCTTTTAGTCAGTGTGGAAAATCTCTAGCAGT-3′). For the Strand-transfer assay the second oligonucleotide lacks GT at the 3′ end. The integrase enzyme was diluted in 750 mM NaCl, 10 mM Tris pH 7.6, 10% glycerol and 1 mM β-mercapto ethanol. To perform the reaction 4 μl diluted integrase (corresponding to a concentration of 1.6 μM) and 4 μl of annealed oligonucleotides (7 nM) was added in a final reaction volume of 40 μl containing 10 mM $MgCl_2$, 5 mM DTT, 20 mM HEPES pH 7.5, 5% PEG and 15% DMSO. The reaction was carried out for 1 h at 37 °C. Reaction products were denatured with 30 mM NaOH and detected by an immunosorbent assay on avidin coated plates.[45]

4.3.42. In vitro anti-HIV and drug-susceptibility assays

The inhibitory effect of antiviral drugs on the HIV-induced cytopathic effect (CPE) in human lymphocyte MT-4 cell culture was determined by the MT-4/MTT-assay.[39] This assay is based on the reduction of the yellow colored 3-(4,5-dimethylthiazol-2-yl)-2,5-diphenyltetrazolium bromide (MTT) by mitochondrial dehydrogenase of metabolically active cells to a blue formazan derivative, which can be measured spectrophotometrically. The 50% cell culture infective dose ($CCID_{50}$) of the HIV(III_B) strain was determined by titration of the virus stock using MT-4 cells. For the drug-susceptibility assays, MT-4 cells were infected with 100–300 $CCID_{50}$ of the virus stock in the presence of fivefold serial dilutions of the antiviral drugs. The concentration of the various compounds that achieved 50% protection against the CPE of the different HIV strains, which is defined as the EC_{50}, was determined. In parallel the 50% cytotoxic concentration (CC_{50}) was determined.

Acknowledgment

This work was supported by THINC project (European commission HEALTH-F3-2008-201032).

References and notes

1. Wallace, A. C.; Laskowski, R. A.; Thornton, J. M. *Protein Eng.* **1995**, *8*, 127.
2. Daria Hazuda, M. I.; Wenning, Larissa *Annu. Rev. Pharmacol. Toxicol.* **2008**, *49*, 377.
3. LaFemina, R. L.; Schneider, C. L.; Robbins, H. L.; Callahan, P. L.; LeGrow, K.; Roth, E.; Schleif, W. A.; Emini, E. A. *J. Virol.* **1992**, *66*, 7414.
4. Anthony, N. J. *Curr. Top. Med. Chem.* **2004**, *4*, 979.
5. Asante-Appiah, E.; Skalka, A. M. *Adv. Virus Res.* **1999**, *52*, 351.
6. Lubkowski, J.; Dauter, Z.; Yang, F.; Alexandratos, J.; Merkel, G.; Skalka, A. M.; Wlodawer, A. *Biochemistry* **1999**, *38*, 15060.
7. Kawasuji, T.; Yoshinaga, T.; Sato, A.; Yodo, M.; Fujiwara, T.; Kiyama, R. *Bioorg. Med. Chem.* **2006**, *14*, 8430.
8. Marchand, C.; Johnson, A. A.; Karki, R. G.; Pais, G. C.; Zhang, X.; Cowansage, K.; Patel, T. A.; Nicklaus, M. C.; Burke, T. R., Jr.; Pommier, Y. *Mol. Pharmacol.* **2003**, *64*, 600.
9. Grobler, J. A.; Stillmock, K.; Hu, B.; Witmer, M.; Felock, P.; Espeseth, A. S.; Wolfe, A.; Egbertson, M.; Bourgeois, M.; Melamed, J.; Wai, J. S.; Young, S.; Vacca, J.; Hazuda, D. J. *Proc. Natl. Acad. Sci. U.S.A.* **2002**, *99*, 6661.
10. Espeseth, A. S.; Felock, P.; Wolfe, A.; Witmer, M.; Grobler, J.; Anthony, N.; Egbertson, M.; Melamed, J. Y.; Young, S.; Hamill, T.; Cole, J. L.; Hazuda, D. J. *Proc. Natl. Acad. Sci. U.S.A.* **2000**, *97*, 11244.
11. Marinello, J.; Marchand, C.; Mott, B. T.; Bain, A.; Thomas, C. J.; Pommier, Y. *Biochemistry* **2008**, *47*, 9345.
12. Pommier, Y.; Johnson, A. A.; Marchand, C. *Nat. Rev. Drug Disc.* **2005**, *4*, 236.
13. Pommier, Y.; Cherfils, J. *Trends Pharmacol. Sci.* **2005**, *26*, 138.
14. Cotelle, P. *Recent Pat. Antiinfect Drug Discov.* **2006**, *1*, 1.
15. Dayam, R.; Gundla, R.; Al-Mawsawi, L. Q.; Neamati, N. *Med. Res. Rev.* **2008**, *28*, 118.
16. Dayam, R.; Deng, J.; Neamati, N. *Med. Res. Rev.* **2006**, *26*, 271.
17. Dayam, R.; Neamati, N. *Curr. Pharm. Des.* **2003**, *9*, 1789.
18. Johnson, A. A. M. C.; Pommier, Y. *Curr. Top. Med. Chem.* **2004**, *4*, 1059.
19. Temesgen, Z.; Siraj, D. S. *Ther. Clin. Risk Manag.* **2008**, *4*, 493.
20. Evering, T. H.; Markowitz, M. *Expert Opin. Invest. Drugs* **2008**, *17*, 413.
21. Summa, V.; Petrocchi, A.; Bonelli, F.; Crescenzi, B.; Donghi, M.; Ferrara, M.; Fiore, F.; Gardelli, C.; Gonzalez Paz, O.; Hazuda, D. J.; Jones, P.; Kinzel, O.; Laufer, R.; Monteagudo, E.; Muraglia, E.; Nizi, E.; Orvieto, F.; Pace, P.; Pescatore, G.; Scarpelli, R.; Stillmock, K.; Witmer, M. V.; Rowley, M. *J. Med. Chem.* **2008**, *51*, 5843.
22. Al-Mawsawi, L. Q.; Al-Safi, R. I.; Neamati, N. *Expert Opin. Emerg. Drugs* **2008**, *13*, 213.
23. Barreca, M. L.; Ferro, S.; Rao, A.; De Luca, L.; Zappala, M.; Monforte, A. M.; Debyser, Z.; Witvrouw, M.; Chimirri, A. *J. Med. Chem.* **2005**, *48*, 7084.
24. Ferro, S.; Barreca, M. L.; De Luca, L.; Rao, A.; Monforte, A. M.; Debyser, Z.; Witvrouw, M.; Chimirri, A. *Arch. Pharm. (Weinheim)* **2007**, *340*, 292.
25. De Luca, L.; Barreca, M. L.; Ferro, S.; Iraci, N.; Michiels, M.; Christ, F.; Debyser, Z.; Witvrouw, M.; Chimirri, A. *Bioorg. Med. Chem. Lett.* **2008**, *18*, 2891.
26. McColl, D. J.; Chen, X. *Antiviral Res.* **2010**, *85*, 101.
27. Barreca, M. L.; Ortuso, F.; Iraci, N.; De Luca, L.; Alcaro, S.; Chimirri, A. *Biochem. Biophys. Res. Commun.* **2007**, *363*, 554.
28. Barreca, M. L.; De Luca, L.; Iraci, N.; Chimirri, A. *J. Med. Chem.* **2006**, *49*, 3994.
29. Barreca, M. L.; Rao, A.; De Luca, L.; Zappala, M.; Monforte, A. M.; Maga, G.; Pannecouque, C.; Balzarini, J.; De Clercq, E.; Chimirri, A.; Monforte, P. *J. Med. Chem.* **2005**, *48*, 3433.
30. Monforte, A. M.; Logoteta, P.; Ferro, S.; De Luca, L.; Iraci, N.; Maga, G.; Clercq, E. D.; Pannecouque, C.; Chimirri, A. *Bioorg. Med. Chem.* **2009**, *17*, 5962.
31. Monforte, A. M.; Rao, A.; Logoteta, P.; Ferro, S.; De Luca, L.; Barreca, M. L.; Iraci, N.; Maga, G.; De Clercq, E.; Pannecouque, C.; Chimirri, A. *Bioorg. Med. Chem.* **2008**, *16*, 7429.
32. Rao, A.; Balzarini, J.; Carbone, A.; Chimirri, A.; De Clercq, E.; Monforte, A. M.; Monforte, P.; Pannecouque, C.; Zappala, M. *Antiviral Res.* **2004**, *63*, 79.

33. Rao, A.; Carbone, A.; Chimirri, A.; De Clercq, E.; Monforte, A. M.; Monforte, P.; Pannecouque, C.; Zappala, M. *Farmaco* **2002**, *57*, 747.
34. Rao, A.; Chimirri, A.; De Clercq, E.; Monforte, A. M.; Monforte, P.; Pannecouque, C.; Zappala, M. *Farmaco* **2002**, *57*, 819.
35. Chen, X.; Tsiang, M.; Yu, F.; Hung, M.; Jones, G. S.; Zeynalzadegan, A.; Qi, X.; Jin, H.; Kim, C. U.; Swaminathan, S.; Chen, J. M. *J. Mol. Biol.* **2008**, *380*, 504.
36. Ferro, S.; De Luca, L.; Barreca, M. L.; Iraci, N.; De Grazia, S.; Christ, F.; Witvrouw, M.; Debyser, Z.; Chimirri, A. *J. Med. Chem.* **2009**, *52*, 569.
37. Murakami, Y.; Tani, M.; Suzuki, M.; Sudoh, K.; Uesato, M.; Tanaka, K.; Yokoyama, Y. *Chem. Pharm. Bull.* **1985**, *33*, 4707.
38. Busschots, K.; Voet, A.; De Maeyer, M.; Rain, J. C.; Emiliani, S.; Benarous, R.; Desender, L.; Debyser, Z.; Christ, F. *J. Mol. Biol.* **2007**, *365*, 1480.
39. Pauwels, R.; Balzarini, J.; Baba, M.; Snoeck, R.; Schols, D.; Herdewijn, P.; Desmyter, J.; De Clercq, E. *J. Virol Methods* **1988**, *20*, 309.
40. Barreca, M. L.; Iraci, N.; De Luca, L.; Chimirri, A. *ChemMedChem* **2009**, *4*, 1446.
41. Maestro, version 8.0, Schrodinger, LLC, New York, NY, 2007.
42. Maurin, C.; Bailly, F.; Buisine, E.; Vezin, H.; Mbemba, G.; Mouscadet, J. F.; Cotelle, P. *J. Med. Chem.* **2004**, *47*, 5583.
43. Sherman, W.; Day, T.; Jacobson, M. P.; Friesner, R. A.; Farid, R. *J. Med. Chem.* **2006**, *49*, 534.
44. Schrçdinger Suite 2007, S., LLC, New York, NY (USA) 2007.
45. Hwang, Y.; Rhodes, D.; Bushman, F. *Nucleic Acids Res.* **2000**, *28*, 4884.
46. DeLano, W. L. The PyMOL Molecular Graphics System. DeLano Scientific LLC, San Carlos, CA, USA. http://www.pymol.org.